Equilibrium melting of plasmid ColE1 DNA: electron-microscopic visualization

A.S.Borovik, Yu.A.Kalambet, Yu.L.Lyubchenko, V.T.Shitov and Eu.I.Golovanov

Institute of Molecular Genetics, USSR Academy of Sciences, Kurchatov Sq., 46, Moscow 123182, USSR

Received 10 April 1980

ABSTRACT

The fine structure of the melting curve for the linear ColE1 DNA has been obtained. To find the ColE1 DNA regions corresponding to peaks in the melting curve's fine structure, we fixed the melted DNA regions with glyoxal /12/. Electron-microscopic denaturation maps were obtained for nine temperature points within the melting range. Thereby the whole process of ColE1 DNA melting was reconstructed in detail. Spectrophotometric and electron microscopic data were used for mapping the distribution of GC-pairs over the DNA molecule. The most AT-rich DNA regions (28 and 37% of GC-pairs), 380 and 660 bp long resp., are located on both sides of the site of ColE1 DNA's cleavage by EcoR1 endonuclease. The equilibrium denaturation maps are compared with maps obtained by the method of Inman /20/ for eight points of the kinetic curve of ColE1 DNA unwinding by formaldehyde.

INTRODUCTION

The studies of DNA melting carried out over the last five years with the use of precision spectrophotometers have revealed some characteristic features of the melting curves of phage DNA /1-6/, the DNA of mitochondria and kinetoplasts /7-9/, namely peaks about 0.3-0.5°C width in the differential melting curve. It was shown in /3/ that peaks appeared in the differential melting curve due to the co-operative melting of DNA regions 300-500 bp long. This explanation was later confirmed by a direct comparison of the theoretical and experimental melting curves for the replicative DNA forms of phages øX 174 /6/ and fd /10/ whose nucleotide sequences were known.

Computation of the melting curves for DNA with a known sequence /6/ shows that the fine structure of the melting

curve is sensitive to slight changes in the nucleotide sequences. Therefore a comparison of the fine structure peaks with the melting regions opens up good prospects for research into the primary structure of DNA with a unknown nucleotide sequence.

The precision equipment available at a number of laboratories for DNA melting studies makes it possible to obtain a highly accurate fine structure of the melting curves. The vast amount of experimental data accumulated on the fine structure of melting curves for different DNAs is summed up in a review by Wada,A. et al. /11/. Meanwhile there is no reliable experimental procedure for localising DNA regions corresponding to the fine structure peaks.

In the present study we fixed the melted regions with glyoxal to determine the ColE1 regions whose melting corresponded to peaks in the fine structure of the melting curve. This method had earlier been used for localizing the AT-rich regions in T7 DNA revealed by the fine structure of the melting curves /12/. Glyoxal reacts with the amino-and imino-groups of bases and prevents complementary pairing; the product of its reaction with guanine is highly stable /13/.

Glyoxal was used to fix the denatured regions appearing in DNA molecules at pre-chosen temperatures within the melting range. The set of denaturation maps subsequently constructed from electron micrographs made it possible to determine the size and location of the DNA regions corresponding to peaks in the fine structure of the melting curve. A combination of spectrophotometry and electron-microscopic visualization of the partially denatured molecules reveals the complete picture of the heat denaturation process. Using these results we constructed a map of the distribution of averaged GC-pair content over the ColE1 DNA molecule.

MATERIALS AND METHODS

1. DNA. A cleared lysate of E.coli C600 cells was obtained by the method of /14/. The major part of chromosome DNA was eliminated by isopropanol extraction. The supernatant containing plasmid DNA was subjected to RNase treatment

and a subsequent triple phenol extraction. The fraction of superhelical plasmid molecules was obtained by equilibrium CsCl centrifugation of deproteinized DNA in the presence of ethidium bromide. After the dye was eliminated from DNA with isopropanol, the DNA was dialyzed against 0.1xSSC for 24 hours with a triple change of buffer. The DNA was purified of short DNA molecules by gel filtration on Sephadex G-50. The DNA preparation thus obtained usually had about a 70% content of superhelical molecules.

2. Restriction endomuclease EcoR1 was obtained as described in /15/.

Endonuclease SmaI was kindly supplied by Dr.Naroditskii B.S. from Ivanovsky Institute of Virology, USSR Academy of Medical Sciences.

The cleavage of ColE1 DNA with EcoR1 endomuclease was carried out at 37°C in a solution containing 100 mM Tris-HCl, 50 mM NaCl and 10 mM $MgCl_2$,pH 7.8. The conditions for endomuclease SmaI were: 15 mM Tris-HCl, 6 mM $MgCl_2$, 15 mM KCl, pH 9.0. The reaction was carried out at 30°C. The resulting linear DNA was purified with phenol. In both cases the reaction was performed for the minimum time required for converting all the molecules to the linear form. These cleavage conditions were chosen to minimize the number of additional sifigle-stranded DNA breaks occuring due to nonspecific nuclease activity. The average number of random single- and double-stranded breaks per DNA molecule was controlled by means of electron microscopy.

3. For the most part DNA melting was carried out on an Opton PMQ III single-beam spectrophotometer equipped with a thermostated cell holder specially designed for precision melting experiments. The melting curves were recorded during continuous heating at a rate of 0.15-0.2 degrees/min. by a two-coordinate recorder, the X coordinate getting the signal from a battery of thermocouples built in the spectrophotometer cell holder. The spectrophotometric accuracy was $2 \cdot 10^{-4}$ optical units for an absorpancy range of 0.5 optical units.

Several experiments were carried out on Cary 219 precision double-beam spectrophotometer equipped with a thermal

unit for DNA melting and a specially designed thermostated cell holder.

4. The differentiation of the experimental melting curves with respect to temperature was carried out by means of a HP9864A digitizer connected to a HP 9825A calculator (Hewlett--Packard, USA). The curve resulting from the digital differentiation was smoothed by convolution with a Gaussian function having a variance of 0.06°C.

5. Melted ColE1 DNA regions were fixed with glyoxal as described in /12/. The cell containing DNA was placed in the spectrophotometer cell holder and heated to a temperature corresponding to a chosen fixation point on the melting curve. Then the first stage of fixation was performed by adding to 0.5 ml of DNA 1 μl of 0.2M glyoxal purified on an Amberlit AG MB-I ion-exchanger resin. The fixation was carried out for 20 minutes and checked by the fact that the DNA absorbancy remained unchanged after a 1°C temperature decrease. The second stage was performed with a higher glyoxal concentration (10 μl to 0.5ml of DNA) for 30-40 minutes. At this stage DNA unwinding by glyoxal was prevented by a gradual temperature decrease. The increase in DNA absorbance due to glyoxal-induced unwinding was insignificant even at the late melting stages as compared with the melting-induced effect.

6. DNA unwinding by formaldehyde was carried out in a solution containing 20-25 μg/ml DNA, 50 mM Na_2CO_3, 5 mM Na_3EDTA, 8.7 mM NaCl, 0.87 mM sodium citrate and 10% formaldehyde. By adding 1M NaOH pH was brought to 10.8-10.85. The reaction was carried out at 24°C; its course was followed by the absorbance at λ =260 nm. Samples were taken at specified intervals and at once prepared for electron microscopy.

7. DNA was prepared for electron microscopy by a modified formamide procedure /16/.

Hyperphase composition: 0.015M phosphate buffer (pH 7.0) 0.01M Na_3EDTA, 65% formamide, 200-300 μg/ml cytochrome C with 3-5 μg/ml DNA.

The concentration of Na^+ in the hyperphase was 0.06 M. The hypophase was deionized water. The preparation was contrasted by circular Pt shadowing at an angle of 7°. Micro-

graphs were obtained on a JEM-7 electron microscope (JEOL, Japan) with a magnification of 8-10 thousand. DNA length was measured with a HP 9864A digitizer connected to a HP 9825A calculator or directly from EM negatives using a PAUK-221 digitizer (USSR) and an EC1010 computer (Hungary). The accuracy of the measurements was about 1%. Partly denatured molecules were analysed and denaturation maps constructed using an HP9825A calculator. The description of the algorithm used for constructing denaturation maps and the program for HP 9825A opt 002 calculator can be sent on request.

RESULTS

a) ColE1 DNA melting and fixation of melted regions.

The melting curves of closed circular DNA do not possess a fine structure /3/, therefore all studies were carried out on linear molecules obtained by single-site cleavage with restriction endonucleases EcoR1 or Sma1. Figure 1 shows the

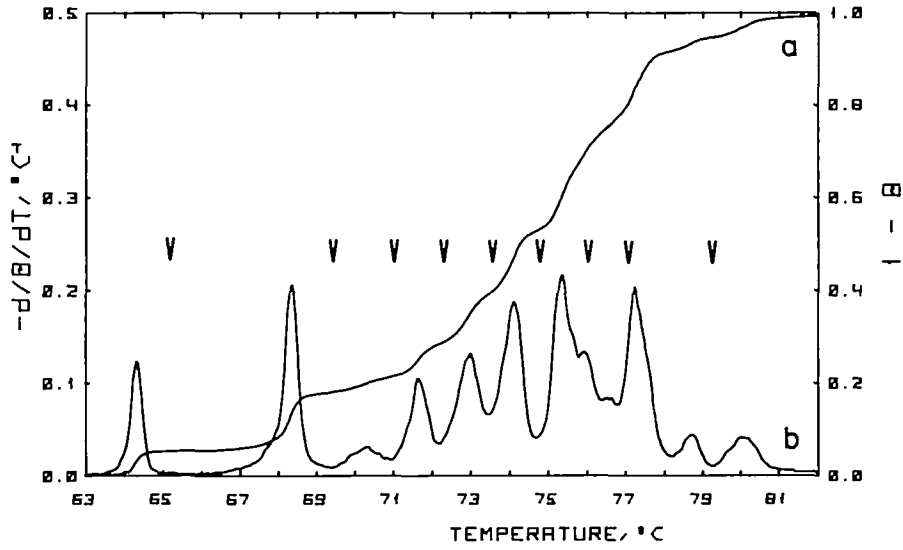

FIGURE 1. The melting curve (a) and the differential melting curve (b) of ColE1 DNA in 0.1xSSC. Arrows indicate the temperatures of fixation. The melting was recorded by the value of absorbancy at λ = 270 nm. The curves presented were obtained by averaging six experimental melting curves.

melting curve (a) of a linear ColE1 DNA molecule obtained by cleavage with EcoR1 and a temperature derivative of that curve - the differential melting curve (b). The differential melting curve of ColE1 DNA has a number of clear-cut peaks, most of which are 0.4-0.6°C width. To find out which DNA regions correspond to peaks in the fine structure of its differential melting curve, we fixed partly denatured molecules with glyoxal at nine chosen temperatures within the melting range. These points are indicated by arrows in Figure 1; they usually fell between adjacent peaks.

b) Electron microscopic data.

Figure 2 presents the electron micrographs of partly denatured molecules fixed at different melting stages. The melted DNA regions are indicated by arrows. One can see that molecules fixed at different temperatures differ in the number of melted regions and/or their size. Table 1 presents

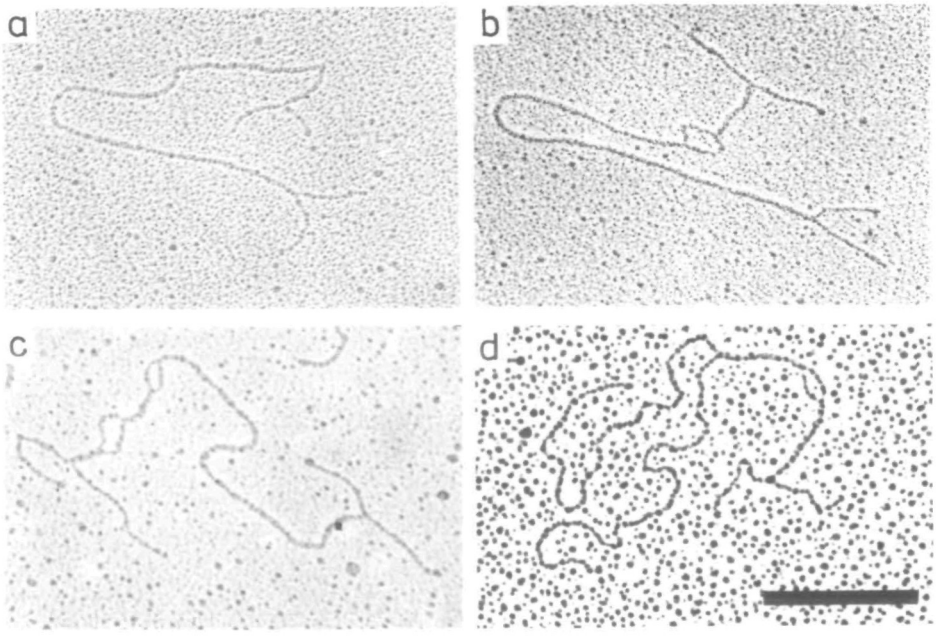

FIGURE 2. Micrographs of partly denatured ColE1 DNA molecules fixed at 69.3°C (a), 71°C (b), 72.2°C (C), 74.7°C (d). Arrows show the denaturated regions. The bar represents 0.4 μm.

Table 1. Characteristics of the arrays of molecules used for electron-microscopic mapping of equilibrium melting.

Temperature of fixation °C	Number of molecules	Average degree of denaturation according to electron microscopy %	Degree of denaturation according to melting curve %
65.0	55	6.5 ± 1.2	5.6
69.3	55	15.7 ± 1.4	18.1
71.0	49	23.9 ± 2.0	21.7
72.2	50	29.0 ± 2.1	28.7
73.5	63	39.3 ± 2.7	39.4
74.7	50	55.1 ± 2.9	52.9
75.9	55	71.1 ± 3.7	70.2
77.0	58	82.0 ± 3.1	79.3
78.8	66	95.8 ± 1.5	94.8

some averaged characteristics of the molecules. For comparison the same table shows the spectrophotometric values of the degree of denaturation for each fixation point. The good agreement of electron microscopic and spectrophotometric data demonstrates that with the above fixation procedure the electron microscopic visualization of partly denatured molecules gives an adequate picture of DNA melting. For each melting stage about 50 DNA molecules were measured and computer-oriented for the subsequent construction of denaturation maps. Figure 3 shows an array of molecules fixed at a temperature of 74.6°C corresponding to 55.4% denaturation degree. The denaturation map obtained by a summation of these molecules is presented in Figure 4f. It should be noted that the short helical section between two long denatured regions at the right-hand end of the molecule (region 80–82) is present in almost all the molecules of the array. The experimental error in determining the coordinates of the ends of this section

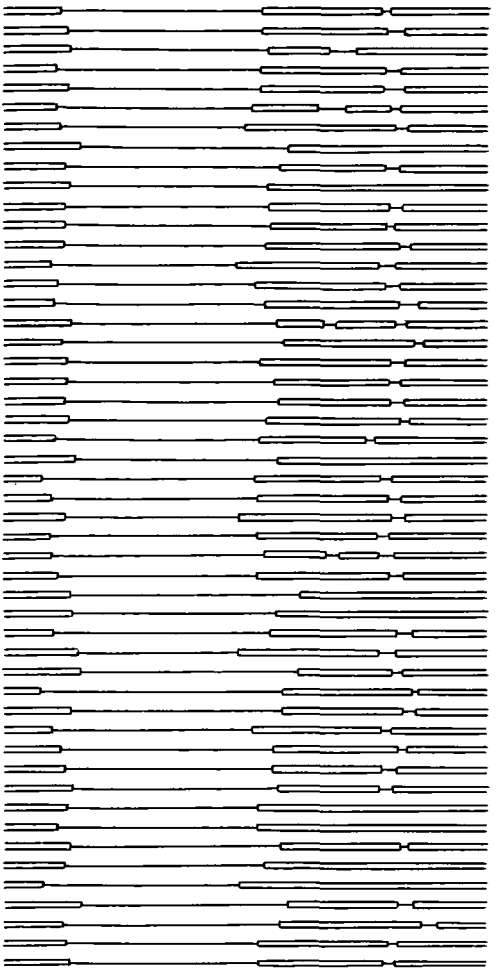

FIGURE 3. The set of molecules used for constructing the denaturation map corresponding to T_f=74.7°C.

accounts for the fact that only a small minimum corresponds to it in the denaturation map (Fig.4f).

c) Denaturation maps of various melting stages. The melting pattern of ColE1 DNA.

Figure 4 presents the denaturation maps corresponding to all the nine points within the colE1 DNA melting range

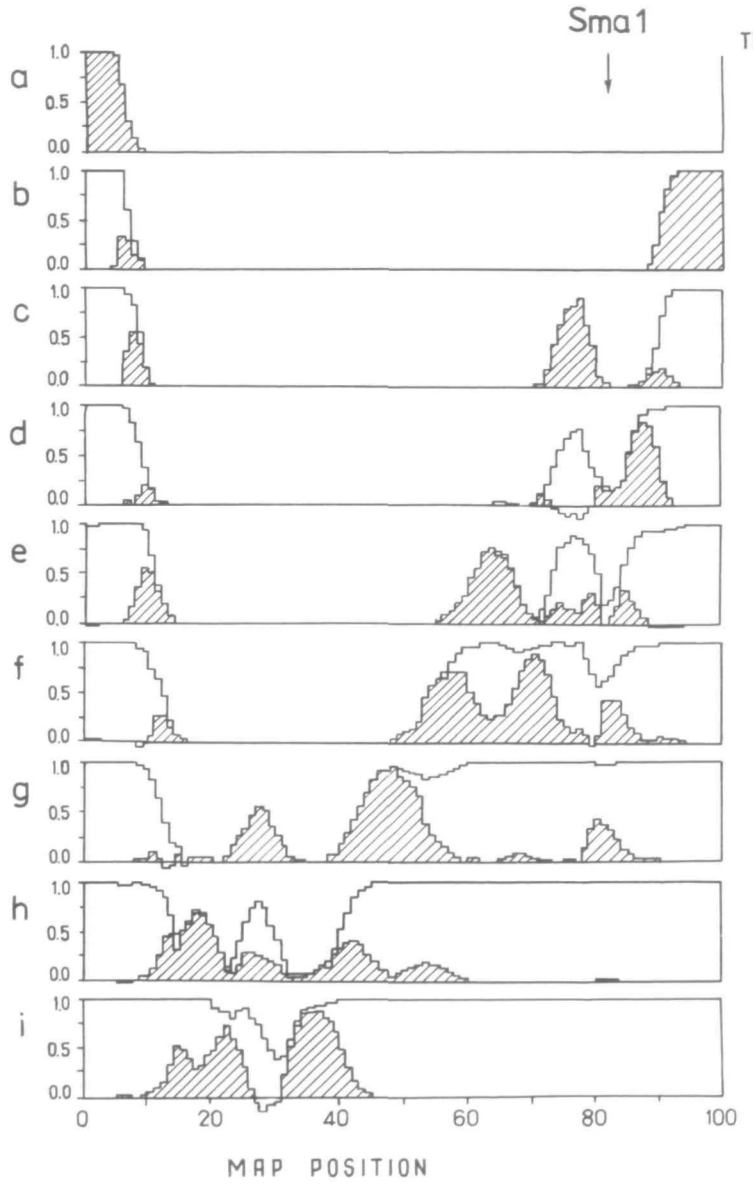

FIGURE 4. Denaturation maps of ColE1 DNA corresponding to different melting stages. The shaded area in each map is the difference obtained by subtracting from this map the map for the preceding temperature of fixation. The temperatures, T_f, are shown on the right. The arrow indicates the cleavage site for Sma1 endonuclease.

indicated by arrows in Figure 1. When analysing the melting of ColE1 DNA it is convenient to compare not only these denaturation maps corresponding to the various melting stages but also difference maps obtained by subtracting the preceding histogram from the following one. Such difference maps of denaturation show which DNA regions correspond to each peak in the fine structure of the melting curve. The maps presented demonstrate that each peak in the fine structure corresponds to the melting of one or several DNA regions. For instance, the first two peaks correspond to the melting of the two terminal regions of the linear ColE1 DNA molecule obtained by EcoR1 cleavage. (In a circular ColE1 DNA molecule the first two melting regions lie on both sides of the EcoR1 site. These data are confirmed by the denaturation maps for a linear DNA molecule obtained by Sma1 cleavage. (Data not shown).)

The melting regions may be located in the long helical region (e.g. Fig.4c, region 74.1-79.1; Fig.4e, region 61-66.7), at the end of the melted region (e.g. Fig. 4c, region 6-8.6; Fig. 4d, region 85.3-89.7) or between two melted regions (e.g. Fig. 4f, region 66.7-73.4). One can see that the peaks in the denaturation maps are of the same height, close to 1, i.e. the denatured regions corresponding to each peak are present in practically all the molecules of the array (see Fig.3). Region 25-29 in Figure 4g is an exception. This region is not to be found in all the molecules of the array because the temperature of fixation, 75.9°C, corresponds to the middle of this region's melting range (see Fig.1). The last map (4i) shows that the intensive peak at T=77.3°C and the next one (see Fig.1b) are due to the melting of three helical regions. The same map demonstrates that the DNA strands are prevented from completely strand separation by region 29-32.

In the denaturation maps the site for Sma1 endonuclease is in the right-hand part of the DNA molecules at a distance of 18.5% from the right end. (In case of successive cleavage by EcoR1 and Sma1 enzymes the resulting DNA fragments are 81.5% and 18.5% of ColE1 genome length) To orient the maps

presented in Fig.4 with respect to the functional map of the plasmid the denaturation maps corresponding to the first three peaks in differential melting curve of the Sma1-cleaved DNA were constructed. (Data not shown).

d) The map of averaged GC-content.

The above analysis allowed a detailed reconstruction of DNA melting and the identification of the co-operatively melting regions corresponding to all peaks in the differential melting curves of ColE1 DNA.

Table 2 specifies the size of these regions, their co-or-

Table 2. Temperatures of melting and sizes of the co-operatively melting regions of ColE1 DNA.

Co-ordinates of the melting region	Size bp	Temperature °C
0.0 - 6.0	380	64.3
6.0 - 8.6	170	68.4
9.1 - 11.3	140	73.0
12.3 - 14.0	110	76.6
14.0 - 16.3	150	77.4
16.3 - 20.3	260	77.3
20.3 - 25.0	300	78.7
25.0 - 29.0	250	76.0
29.0 - 32.0	190	80.1
32.0 - 40.4	540	77.3
40.4 - 43.3	190	76.6
43.3 - 54.2	700	75.4
54.2 - 61.0	440	74.1
61.0 - 66.7	360	73.0
66.7 - 73.4	430	74.1
74.1 - 79.1	320	70.3
80.1 - 82.8	170	75.4
82.8 - 84.4	100	74.1
85.3 - 89.7	280	71.7
89.7 - 100	660	68.4

dinates in the DNA molecule and the melting temperatures corresponding to the maximum of the relevant peaks in the differential melting curve (see Figures 1 and 4).

These data were used for computing the average content of GC-pairs in each melting region. The GC content was computed on the basis of the well-known Marmur and Doty's relation /17/, making allowance for the boundary melting conditions of each region /12,24,25/. The distribution of GC-pairs over the ColE1 DNA molecule is presented in the form of a histogram in Figure 5. Below is a functional map of the ColE1 plasmid taken from /18/.

Figure 5 shows that ColE1 DNA is characterized by considerable intramolecular heterogeniety. Along with a highly AT-rich region at the left end of the DNA molecule (28% of GC-pairs), there is the highly GC-rich region 29.0-32 (73% of GC-pairs). The melting of this region causes a complete separation of the DNA strands (the last peak in the melting curve), so that the above figure is only a rough estimate of its GC content.

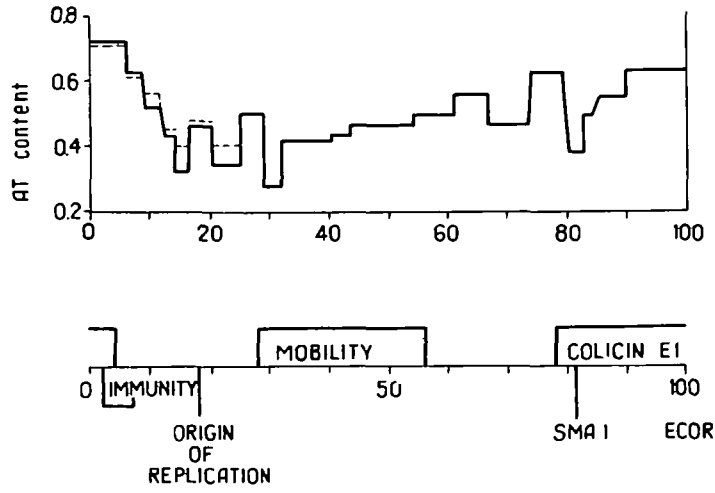

FIGURE 5. The distribution of AT-pairs over the ColE1 DNA molecule. (solid line) Dashed line represents the average AT content of the appropriate regions of pA02 DNA /23/ (see text). Shown below is a functional map of the plasmid ColE1 /18/.

•) Formaldehyde maps

Denaturation mapping of DNA with formaldehyde as the denaturing agent has become a common technique over the last decade /19-21/. To compare the data yielded by formaldehyde maps with the equilibrium melting maps obtained in the present study, we performed denaturational mapping of the various stages of ColE1 DNA unwinding kinetics induced by formaldehyde at pH10.8, T=24°C. (The denaturation maps are more distinct in these conditions than at neutral pH /20/.) The denaturation maps are shown in Figure 6. Table 3 gives the characteristics of the arrays of molecules used for constructing these maps.

Figure 6 shows that formaldehyde starts by unwinding the left end of the DNA molecule. This process seems to correspond to the steep beginning of the kinetic curve. Then the right end begins unwinding (Fig.6b). Meanwhile the left-hand denatured region increases in size. Long-time denaturation maps show that regions in the right half of the DNA molecule are unwound next (Fig.6c,d), and only then the left half of the molecule (Fig.6f,g). These data show that the formaldehyde-induced unwinding of different ColE1 DNA regions occurs unevenly and depends on their GC content. Figure 7 presents the kinetic curves of unwinding of ColE1 DNA regions differing in the average GC content computed from the equilibrium denaturation maps. The kinetic curves were obtained by computing the average denaturation degree of the DNA regions from the relevant denaturation maps. One can see that the AT-rich regions are the first to unwind and do so at a higher rate. This dependence of the formaldehyde-induced unwinding of a DNA region on its GC content accounts for the similarity between the formaldehyde maps and the equilibrium melting maps. This similarity, however, is only observed at the early stages of the unwinding kinetics before any significant proliferation of the unwound regions occurs.

Differences in the rate of unwinding between different regions of λ phage DNA were first revealed by Inman in his early works on formaldehyde denaturation mapping /19,20/. In /21/ a correlation was established between denaturation maps

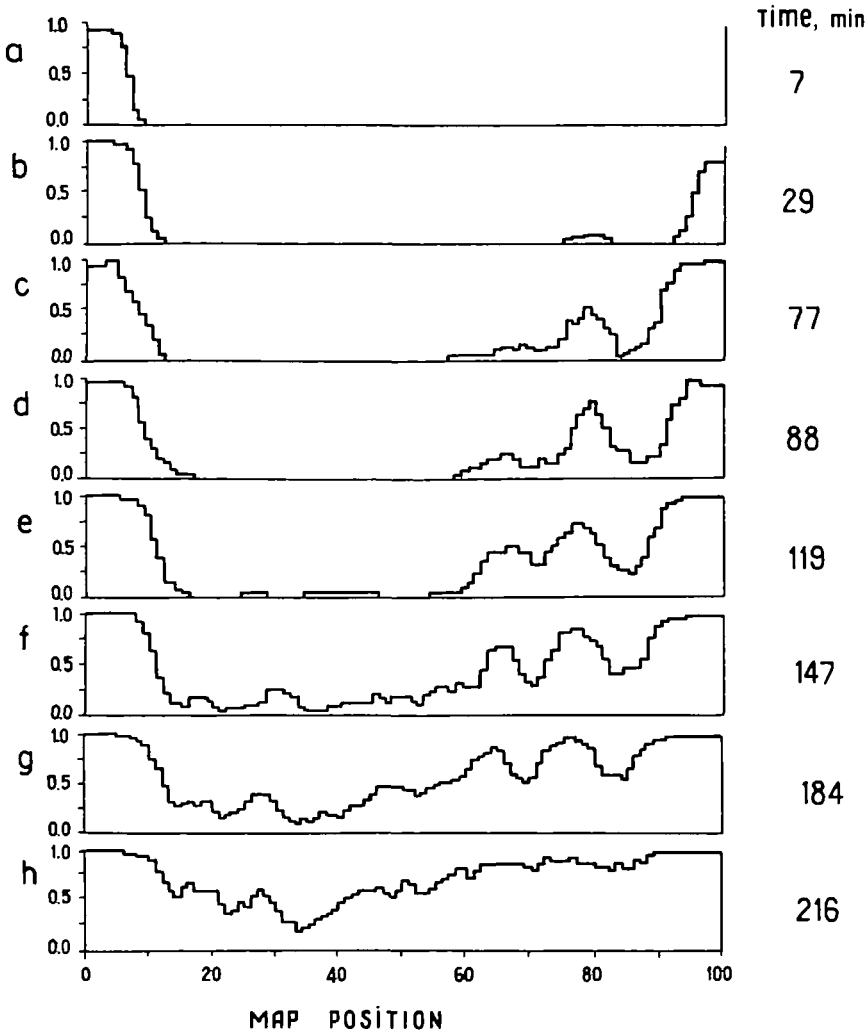

FIGURE 6. Formaldehyde denaturation maps corresponding to different times after the onset of the unwinding reaction. The times are shown on the right.

and maps of averaged GC content through analysis of denaturation maps for DNA with a known nucleotide sequence: φX174 and SV40.

A comparison of formaldehyde denaturation maps with

Table 3. Characteristics of the arrays of partly denatured molecules used for formaldehyde denaturation mapping.

Time since onset of kinetics min	Degree of denaturation according to EM %	Number of molecules
7	6	40
29	13	50
77	23	31
88	27	23
129	34	48
147	45	43
184	60	66
216	74	51

equilibrium ones shows that the sequence of unwinding of DNA regions 300-500 bp long corresponds to peaks in the melting curve's fine structure. This correlation is also noted in /22/ where it is derived from a comparison between an experimental formaldehyde denaturation map of replicative form of φX174 DNA and a melting map computed for that DNA on the basis of the theory.

The partly denatured DNA molecules obtained by formaldehyde unwinding show a wider variance in the number of mel-

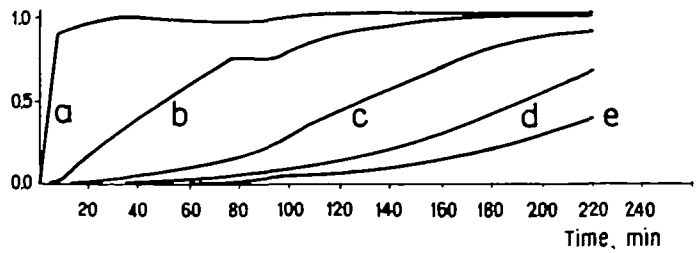

FIGURE 7. Kinetic curves of formaldehyde-induced unwinding for DNA regions with different GC content: 28% (a), 38% (b), 45% (c), 54% (d) and 58% (e).

ted regions and their length (i.e. the degree of denaturation, see also /21/) than the molecules fixed with glyoxal in the course of equilibrium heat melting. For instance, in the array of molecules used for constructing the denaturation map in Figure 6g (degree of denaturation $1-\theta=59.8\%$) the variance in the degree of denaturation is 8.75%. This is reflected in the denaturation maps: the peaks in formaldehyde denaturation maps differ in height and have more blurred boundaries.

DISCUSSION

The glyoxal fixing technique used in the present study made it possible to construct equilibrium melting maps of ColE1 DNA and thereby experimentally visualize the whole process of its melting (Fig.8). The small variation in the number of melted regions and the degree of DNA denaturation as well as the agreement between this value and the spectrophotometric data demonstrate that glyoxal fixes partly denatured DNA regions alone under the experimental conditions. The visualization of the melting process shows that the appearance of each sharp peak in the differential melting curve corresponds to the melting of one or several DNA regions several hundred bp long. These data are a direct experimental confirmation of the existing concept as to the origin of the melting curve's fine structure. /3,6/ On the whole the denaturation maps are similar to the theoretical denaturation maps of DNA with a known nucleotide sequence; the replicative forms of fd DNA /10/ and ϕX174 DNA /6/. Analysis of the denaturation maps (Fig.4) shows the melting of most DNA regions to be co-operative. Apart from the co-operative melting, however, there is an appreciably less co-operative process involving the melting of regions several dozen bp long. This kind of melting produces a wide bell-shaped background in the differential melting curve while the sharp peaks standing out against it correspond to the co-operative melting of long regions. The "non-co-operative" melting may be due, for instance, to an even unwinding of the bounda-

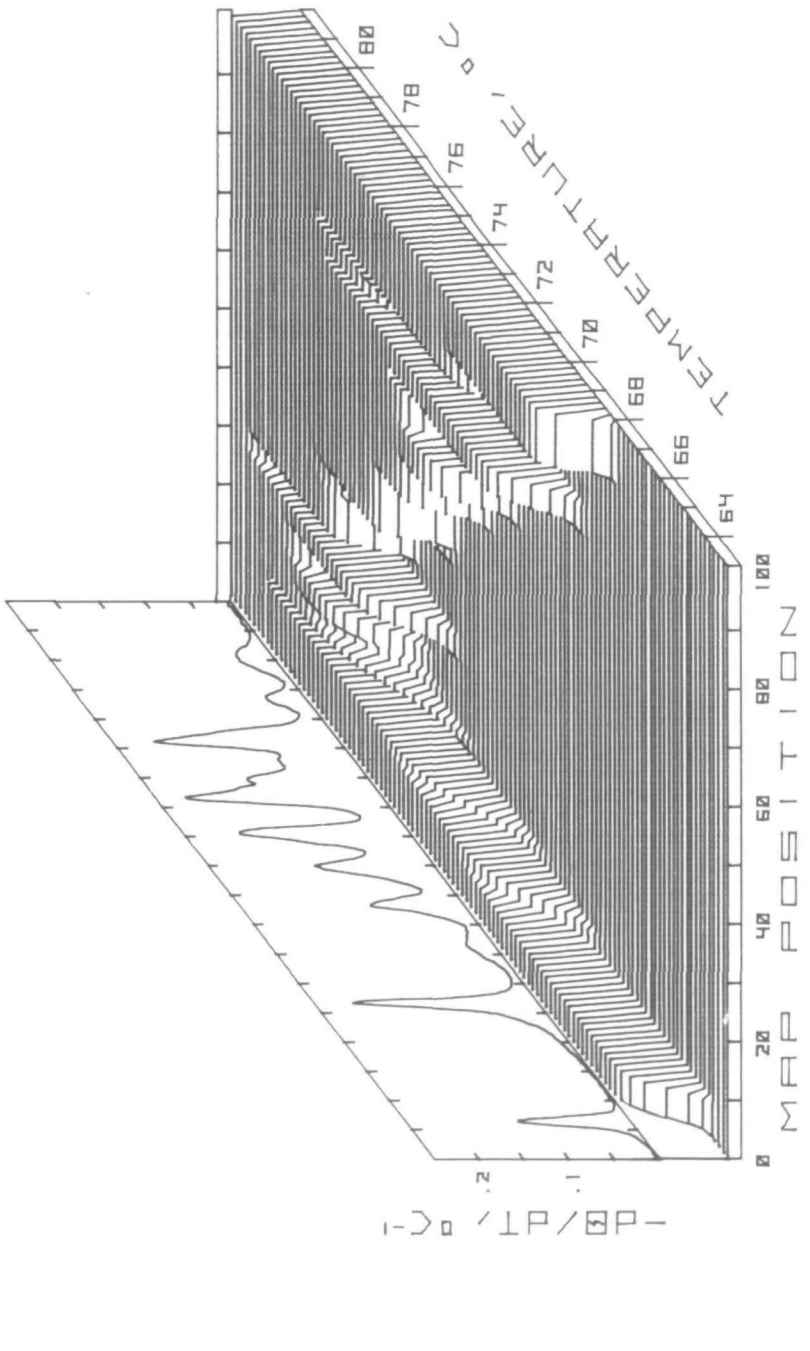

FIGURE 8. The three-dimensional diagram illustrating the process of the heat melting of ColE1 DNA. The Z co-ordinate represents the probability of the melting of a given region of the molecule at different temperatures. For comparison the differential melting curve is shown on the left.

ries of helical regions. Still, analysis of difference denaturation maps shows that the "non-co-operative" proliferation of the denatured regions is not extensive. Of great interest are the short regions that can melt within the helical part of the DNA molecule. Unfortunately such short denatured regions are hard to visualize using the above-described procedure. The melting of short helical regions changes the boundary conditions for the co-operative melting of adjacent regions. But estimations show that the melting of a short region practically does not affect the average GC content of a total DNA region several hundred bp long as determined by the aforesaid procedure. Therefore while determining the GC content of a melting region over 300 bp long, only the state of long adjacent regions should be allowed for, which is easily done from the denaturation maps (Fig.4).

It would be interesting to compare the GC content of the melting regions obtained from the denaturation maps with the nucleotide sequence determined by direct techniques. However, only part of ColE1 DNA has been sequences so far. The largest fragment was described in /23/. The pAO2 plasmid whose sequence was decoded in that study contains 25% of the ColE1 genome. The pAO2 plasmid contains the restriction site for EcoR1 and the ori site of ColE1. In the map of GC content (Fig.5) the pAO2 plasmid corresponds to region 0 - 25 of ColE1 DNA. This region of ColE1 DNA is the most heterogeneous in respect of GC content: it includes both the most AT-rich section and highly GC-enriched sections. The discrepancy in the value of GC content of the two most thermostable regions (14-16.3 and 20.3-25) may be explained by the fact that these regions melt under irreversible conditions to which the formulae used are, strictly speaking, inapplicable. Indeed, the melting process in these conditions (0.1xSSC) is not strictly equilibrium, for in solutions of such low ionic strength there is practically no renaturation of the separated strands at low DNA concentrations /7,8/.

The same may account for the hysteresis of the ColE1 DNA melting curve, i.e. the divergence between the melting curve and the renaturation curve obtained during the gradual

cooling of DNA melted to degree of denaturation approx.0.5 /11/. Indeed, at T=74.2°C, which corresponds degree of denaturation 1-θ=0.52, the section of ColE1 DNA lying between two melted regions melts for the first time (Fig.4d, 4c). If the temperature is lowered after that, this section, now part of a long melted region, must be the first to renature. The process is impeded at low ionic strength, hence the "overcooling" of the section resulting in hysteresis. The renaturation of those melted regions that border on the helical parts may start at the ends; this process does not depend on the ionic strength and the melting of such regions is reversible. The melting and renaturation curves coincide for such regions. The denaturation maps in Figure 4a,b,c,d show that the melting of ColE1 DNA under these ionic conditions up to T=73.4°C is fully reversible, which is a fact experimentally observed /11/.

The data on the GC content of various co-operatively melting regions reveal a marked intramolecular heterogeneity of ColE1 DNA. The left-hand terminal region of the linear ColE1 DNA molecule shows the highest AT content (Fig.5). Its GC content is only 28%, about half the average of the DNA molecule. The long region (660 bp) at the right end of the DNA molecule is somewhat richer in GC pairs: its GC content is 37%. In reality ColE1 DNA is a circular molecule, so these two regions lie next to each other on both sides of the cleavage site for EcoR1 endonuclease. In a linear ColE1 DNA molecule the right-hand part is more AT-rich (Fig.5). The most GC-rich regions (average GC content over 60%) are in the left-hand part of the molecule, in the ori region.

ACKNOWLEDGEMENTS

The authors would like to thank Prof. Yu.S.Lazurkin, Dr.M.D.Frank-Kamenetskii and Dr. A.V.Vologodskii for the interest in the work and for stimulating discussions, and Dr. B.S.Naroditskii for the gift of Sma1 endonuclease.

REFERENCES

1. Gomez,B. and Lang,D. (1972) J.Mol.Biol. 70, 236-251.
2. Yabuki,S., Gotoh,O. and Wada,A. (1975) Biochim. Biophys. Acta 395, 258-273.
3. Lyubchenko, Yu.L., Frank-Kamenetskii,M.D., Vologodskii, A.V., Lazurkin, Yu.S. and Gause, G.G. (1976) Biopolymers 15, 1019-1036.
4. Vizard,D.L. and Ansevin,A.T. (1976) Biochemistry 15, 741-750.
5. Tachibana,H., Wada,A., Gotoh, O. and Takanami,M. (1978) Biochim. Biophys. Acta 517, 319-328.
6. Lyubchenko, Yu.L., Vologodskii, A.V. and Frank-Kamenetskii, M.D. (1978) Nature 271, 28-31.
7. Michel,F. (1974) J.Mol.Biol. 89, 305-326.
8. Michel,F., Lasowska,I., Faye,G., Fukuhara,H. and Slonimski,P. P.(1974) J.Mol.Biol. 85, 411-431.
9. Steinert,M. and Van Assel,S. (1974) Biochim. Biophys. Res.Comm. 61, 1249-1255.
10. Vologodskii, A.V. and Frank-Kamenetskii, M.D. (1978) Nucl. Acids Res. 5, 2547-2556.
11. Wada,A., Yabuki,S. and Husumi,Y. (1979) Crit. Rev.Biochem., CRS Press Inc. (in press).
12. Pavlov, V.M., Lyubchenko, Yu.L., Borovik, A.S. and Lazurkin, Yu.S. (1977) Nucl.Acids Res. 4, 4053-4061.
13. Broude,N.E. and Budowsky, E.I. (1973) Biochim. Biophys. Acta 294, 378-384.
14. Clevell, D.B. (1972) J.Bacter. 110, 667-676.
15. Sumegi,J., Breedveld,D., Hossenlopp,P. and Chambon,P. (1977) Biochem. Biophys. Res. Com. 76, 78-85.
16. Davis,R.W., Simon,M. and Davidson,N. (1969) Meth.Enzym. (D) 21, 413-428.
17. Marmur,T. and Doty,P. (1962) J.Mol.Biol. 5, 109-118.
18. Dougan,G., Saul,M., Warren,G. and Sheratt,D. (1978) Molec.Gen.Genet. 158, 325-327.
19. Inman,R.B. (1966) J.Mol.Biol. 18, 464-476.
20. Inman,R.B. and Schnös,M. (1970) J.Mol.Biol. 49, 93-98.
21. Funnel,B.E. and Inman,R.B. (1979) J.Mol.Biol. 131, 331-340.
22. Karataev,G.L., Permogorov,V.I., Vologodskii,A.V. and Frank-Kamenetskii, M.D. (1978) Nucl.Ac.Res. 5, 2493-2500.
23. Oka,A., Nomura,N., Morit,M., Sugisaki,M., Sugimoto,K. and Takanami,M. (1979) M.Gen.Genet. 172, 151-159.
24. Lyubchenko,Yu.L., Trifonov,E.N., Lazurkin,Yu.S. and Frank-Kamenetskii,M.D. (1971) Mol.Biol., 5, 772-774.
25. Azbel,M.Ya. (1979) Proc.Nat.Acad.Sci. USA 76, 101-105.